



SELF-ADAPTIVE FAULT-TOLERANT CONTROL STRATEGY OF SHUNT ACTIVE POWER FILTER BASED ON MULTICELLULAR CONVERTER

Ali BOUHAFS ¹ , Boubakeur ROUABAH ^{2,*} , Mohamed Redouane KAFI ¹ ,
Lakhdar LOUAZENE ¹ 

¹ Laboratoire de Genie Electrique, Kasdi Merbah University, Algeria

² FNTIC Faculty, Kasdi Merbah University, Algeria

* Corresponding author, e-mail: boubakeurrouabah@yahoo.fr

Abstract

The use of multicellular topology in power quality enhancement can reduce the power loss and also dv/dt of power switches, minimize the electromagnetic interference. However, the failure of flying capacitors can reduce the active filtering efficiency and affect the power quality by injecting currents with wave-form distortion (harmonics, notching, noises etc.) in power distribution grid. Therefore, this study presents a fault-tolerant control strategy (FTC) allowing to keep the normal operation conditions of a multicellular converter even under failure mode. The obtained results show that the proposed FTC strategy enhances the power quality of power distribution grid when a fault in flying capacitors occurs.

Keywords: self-adaptive fault-tolerant control, multicellular power converter, shunt active power filter, sliding mode control, power quality improvement

1. INTRODUCTION

Recently, the increasing use of nonlinear loads such as uninterruptible power supplies, adjustable speed drives, furnaces and so on in domestic and industrial appliances, leads to propagate current harmonics in the grid [1-4] and due to the sensitivity of modern industry to power quality problems, these current harmonics can increase the thermal stress, mechanical vibrations, noise in communication systems and electromagnetic interference [5-8]. Shunt Active Power Filters (SAPF) are proposed in many research works in order to solve all these problems, mitigate harmonics and improve power quality [9-12]. The performance of SAPFs depends on the control methods, harmonic detection algorithms; in [13] a pq theory is used to extract harmonics of nonlinear loads and regulate the dc capacitor voltage of, in [14] an active power filter and multicellular topology are used with sliding mode control. In order to exploit the advantageous of neural networks, in [15-19] artificial neural network is applied to three phase shunt active power filter in order to reduce calculation time in estimation of harmonic components. In [20] an artificial neural network method used to drive shunt active power filter for minimizing the harmonic currents in industrial systems, and in [21] the obtained results show the effectiveness of hysteresis current control

to compensate reactive power and mitigate harmonics using shunt active power filter. The performance of SAPF depends also to the topology of power converter used (classical two level converter or multilevel converter).

The multilevel power converters are used in shunt active power filters in order to reduce switching power loss and increase the switching frequency [22-26]; among the multilevel topologies of power converter, flying capacitor or multicellular topology has various advantages in comparison to other multilevel topologies such as small dv/dt , it combine between high switching frequency capability and reduced voltage on the power switches [27]. In [28] an active power filter with multicellular topology proves the robustness against variations of nonlinear load and minimize the switching losses. However, during a failure in power capacitor, the multicellular converter injects faulty current harmonics and affects the power quality of electric power grid, therefore the use of fault tolerant control in modern industry is very important [29-31]. In [32-33] a multicellular converter with fault tolerant control used in wind energy conversion system and solar photovoltaic system.

In this paper, a shunt active power filter with three cells multicellular converter used to enhance power quality of 50 Hz grid, self-adaptive FTC is

proposed to enhance the power quality of electric power grid under failure flying capacitor conditions.

The organization of this paper is as follow: in section-2 material and methods which present the modeling of shunt active power filter based on three cells multicellular converter, sliding mode control is applied in both of healthy and different failure modes of three cells multicellular converter, and the applying of self-adaptive fault tolerant control to proposed topology with one or two flying capacitor failure, in section 3 results and discussion with the comparison between THD values of deferent operating modes of shunt active power filter and finally the conclusion of this work in section 4.

Fig. 1, shows the proposed topology of shunt active power filter.

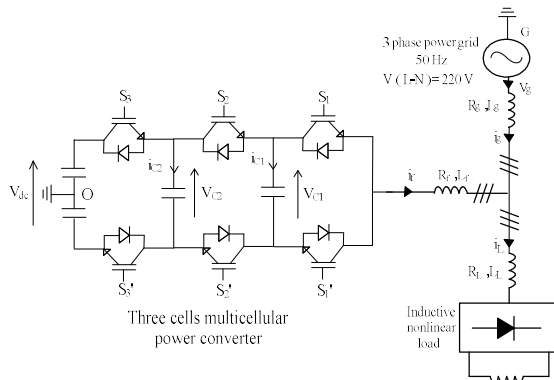


Fig. 1. Proposed topology of shunt active power filter

2. MATERIAL AND METHOD

2.1. Modeling of three cells multicellular power converter

Figure 1 show a three phase shunt active power filter based on multicellular converter, this later topology is used in order to compensate current harmonics generates from inductive nonlinear load [6].

Flying capacitors currents are given by:

$$\begin{aligned} i_{C1} &= C \frac{d}{dt} V_{C1} \\ i_{C2} &= C \frac{d}{dt} V_{C2} \end{aligned} \quad (1)$$

Flying capacitors voltages are expressed by:

$$\begin{aligned} \frac{d}{dt} V_{C1} &= \frac{1}{C} [S_2 - S_1] \\ \frac{d}{dt} V_{C2} &= \frac{1}{C} [S_3 - S_2] \end{aligned} \quad (2)$$

From Figure 1 the output voltage V_{OG} of multicellular converter can be expressed by:

$$V_{OG} = S_1 V_{C1} + S_2 [V_{C2} - V_{C1}] + S_3 [V_{dc} - V_{C2}] \quad (3)$$

Output current of multicellular converter i_f or filter current is given by:

$$\begin{aligned} \frac{di_f}{dt} &= \frac{1}{L_f} (S_1 V_{C1} + S_2 [V_{C2} - V_{C1}] \\ &\quad + S_3 [V_{dc} - V_{C2}]) - \frac{R_f}{L_f} i_f \end{aligned} \quad (4)$$

$$\begin{aligned} -\frac{V_{dc}}{2L_f} - \frac{V_g}{L_f} \\ i_f = i_L - i_g \end{aligned} \quad (5)$$

The nonlinear form of proposed shunt active power filter is:

$$\begin{aligned} \begin{bmatrix} \dot{V}_{C1} \\ \dot{V}_{C2} \\ \dot{i}_f \end{bmatrix} &= \begin{bmatrix} 0 & 0 & 0 \\ 0 & 0 & 0 \\ 0 & 0 & -\frac{R_f}{L_f} \end{bmatrix} \begin{bmatrix} V_{C1} \\ V_{C2} \\ i_f \end{bmatrix} \\ &+ \begin{bmatrix} -\frac{(i_L - i_g)}{C} & \frac{(i_L - i_g)}{C} & 0 \\ 0 & -\frac{(i_L - i_g)}{C} & \frac{(i_L - i_g)}{C} \\ \frac{V_{C1}}{L_f} & \frac{V_{C2} - V_{C1}}{L_f} & \frac{V_{dc} - V_{C2}}{L_f} \end{bmatrix} \begin{bmatrix} S_1 \\ S_2 \\ S_3 \end{bmatrix} \\ &+ \begin{bmatrix} 0 \\ -\frac{V_{dc}}{2L_f} - \frac{V_g}{L_f} \end{bmatrix} \end{aligned} \quad (6)$$

2.2. DC Capacitor voltage regulation

In order to mitigate the harmonic currents of nonlinear load, DC side capacitor must be regulated at fixed voltage V_{dc} [14]. In this work, the instantaneous power theory is used to extract the filter currents references and to regulate the dc side capacitor as detailed in [18].

The filter currents in $\alpha\beta$ frame can be expressed as:

$$\begin{bmatrix} i_{f\alpha ref} \\ i_{f\beta ref} \end{bmatrix} = \frac{1}{V_{g\alpha}^2 + V_{g\beta}^2} \begin{bmatrix} V_{g\alpha} & V_{g\beta} \\ V_{g\beta} & -V_{g\alpha} \end{bmatrix} \begin{bmatrix} \bar{P} - \Delta P \\ \bar{q} + \tilde{q} \end{bmatrix} \quad (7)$$

ΔP : represent the active power necessary to keep the voltage of dc capacitor constant.

The output current i_{fabc} can be expressed as:

$$\begin{bmatrix} i_{fa} \\ i_{fb} \\ i_{fc} \end{bmatrix} = \sqrt{\frac{2}{3}} \begin{bmatrix} 1 & 0 \\ -\frac{1}{2} & \frac{\sqrt{3}}{2} \\ -\frac{1}{2} & -\frac{\sqrt{3}}{2} \end{bmatrix} \begin{bmatrix} i_{f\alpha ref} \\ i_{f\beta ref} \end{bmatrix} \quad (8)$$

2.3. Multicellular Converter with Sliding Mode Control (Healthy mode)

Equation 6 represent a nonlinear model of shunt active power filter based on multicellular converter expressed in can be written as:

$$\dot{x} = f(x) + g(x)u + H \quad (9)$$

With

$x = [V_{C1} \ V_{C2} \ i_f]^T$ is the state vector.

$x_{ref} = [\frac{V_{dc}}{3} \ \frac{2V_{dc}}{3} \ i_{fref}]^T$ reference state vector.

$$f(x) = \begin{bmatrix} 0 & 0 & 0 \\ 0 & 0 & 0 \\ 0 & 0 & \frac{-R_f}{L_f} \end{bmatrix}$$

$$g(x) = \begin{bmatrix} \frac{-(i_L - i_g)}{C} & \frac{(i_L - i_g)}{C} & 0 \\ 0 & \frac{-(i_L - i_g)}{C} & \frac{(i_L - i_g)}{C} \\ \frac{V_{C1}}{L_f} & \frac{V_{C2} - V_{C1}}{L_f} & \frac{V_{dc} - V_{C2}}{L_f} \end{bmatrix}$$

$u=[s_1s_2s_3]^T$ input vector,

$$H = \begin{bmatrix} 0 \\ 0 \\ \frac{-V_{dc}}{2L_f} - \frac{V_g}{L_f} \end{bmatrix} \text{ constant vector.}$$

Where error vector e is expressed by

$$e = x_{ref} - x = \begin{pmatrix} \frac{V_{dc}}{3} - V_{C1} \\ \frac{2V_{dc}}{3} - V_{C2} \\ i_{fref} - i_f \end{pmatrix} \quad (10)$$

In this work, sliding surface is considered as the error vector. Therefore, in order to assure the stability according to LYAPUNOV theory, we define a new positive function V :

$$V = \frac{1}{2} e^T e \quad (11)$$

The first derivation of function V is given in equations (12,13):

$$\dot{V} = e^T \dot{e} \quad (12)$$

$$\dot{V} = e^T (\dot{x} - \dot{x}_{ref})$$

$$\dot{V} = e^T (f(x) + g(x) u + H - \dot{x}_{ref}) \quad (13)$$

The output of sliding mode control:

$$u = u_{eq} + u_n \quad (14)$$

Where the control u_n represent sliding surface sign, u_{eq} is the control which forces the state variables to the origin. u_{eq} led to $e=0$ and " $\dot{e} = 0$ " So,

$$u_{eq} = -(g(x))^{-1} (f(x) + H - \dot{x}_{ref}) \quad (15)$$

$$u = -(g(x))^{-1} (f(x) + H - \dot{x}_{ref}) + u_n \quad (16)$$

According to equations 16 and 13

$$\dot{V} = e^T g(x) u_n \quad (17)$$

$$\dot{V} = e^T \left[\left(\frac{(i_L - i_g)}{C} + \frac{V_{C1}}{L_f} \right) S_1 + \left(\frac{(i_L - i_g)}{C} - \frac{(i_L - i_g)}{C} + \frac{V_{C2} - V_{C1}}{L_f} \right) S_2 + \left(\frac{(i_L - i_g)}{C} + \frac{(V_{dc} - V_{C2})}{L_f} \right) S_3 \right] \quad (18)$$

In order to assure the stability according to Lyapunov theory, derivative of function V must be negative.

$$S_1 = - \text{sign} \left[e^T \left(\frac{(i_L - i_g)}{C} + \frac{V_{C1}}{L_f} \right) \right]$$

$$S_2 = - \text{sign} \left[e^T \left(\frac{(i_L - i_g)}{C} - \frac{(i_L - i_g)}{C} + \frac{V_{C2} - V_{C1}}{L_f} \right) \right] \quad (19)$$

$$S_3 = - \text{sign} \left[e^T \left(\frac{(i_L - i_g)}{C} + \frac{(V_{dc} - V_{C2})}{L_f} \right) \right]$$

Figure 2 shows sliding mode control of shunt active power filter based on multicellular converter.

3. RESULTS AND DISCUSSION

System parameters used in simulation are given in table. 1.

Table 1. Simulation parameters

Parameter	Value
f_g	50 Hz
V_g	220V
V_{deref}	1000V
R_f and L_f	1mΩ and 13mH
R_g and L_g	1mΩ and 0.1 10 ⁻³ mH
R_L and L_L	40Ω and 20mH
C_{dc}	8000μF
C	400μF

Figure 2 shows the total flowchart of proposed system.

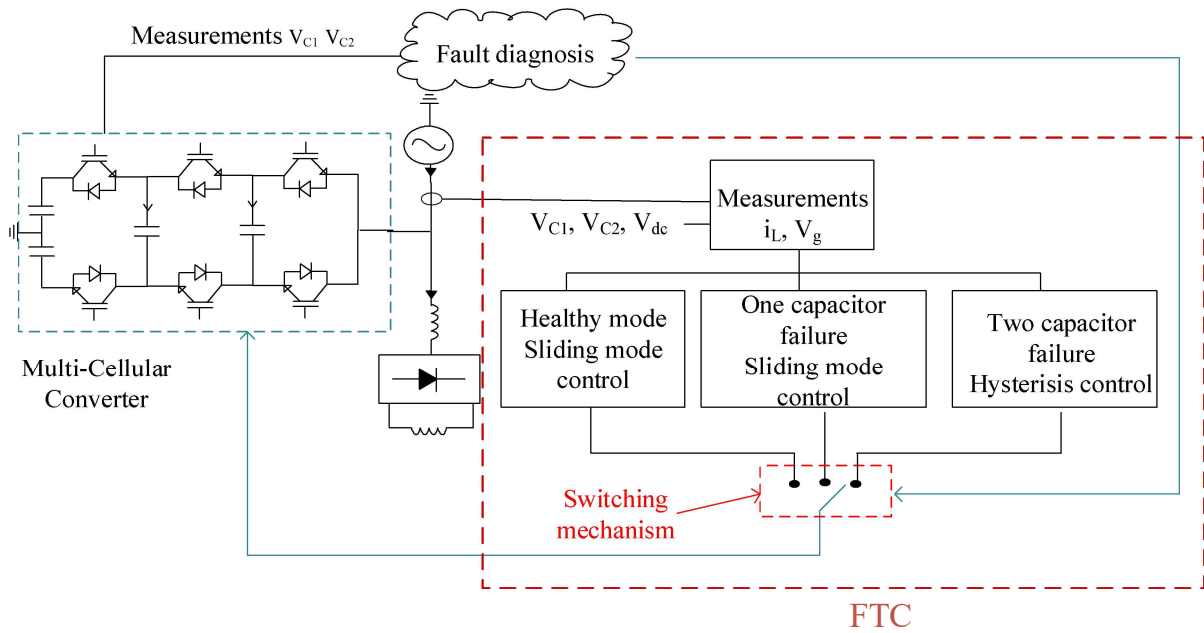


Fig. 2. Total flowchart of proposed system

3.1. Healthy mode operating

Figure 3 shows the sliding mode control of multicellular converter use in shunt active power filter during healthy operation mode.

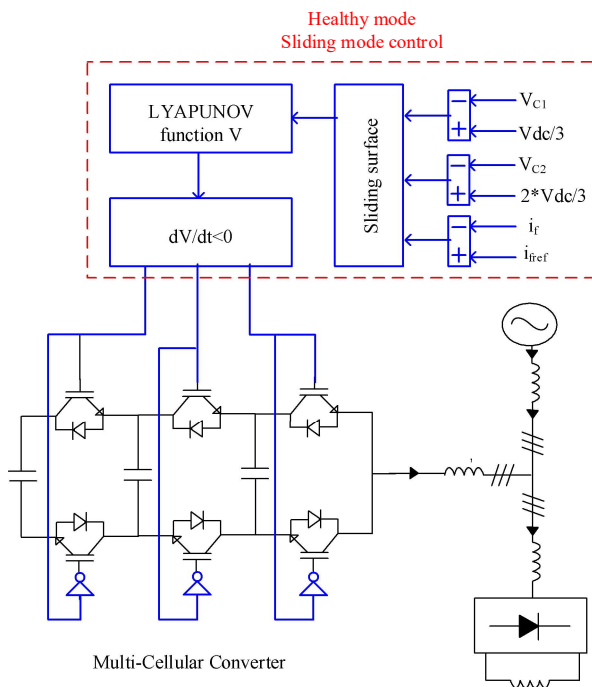


Fig. 3. Multicellular converter with sliding mode control

In healthy mode operation the dc side voltage is regulated at $V_{dc}=1000V$ which equal to $V_{dcref}=1000V$ and the flying capacitors are regulated at their references $V_{C1}=V_{C1ref}=V_{dc}/3$ and $V_{C2}=V_{C2ref}=2*V_{dc}/3$ as represented in Figure 4. In the Figure 5 the nonlinear load current is deformed and

not sinusoidal, the current generated by multicellular converter is given in figure 6. The multicellular converter assure a sinusoidal current in power grid with $THD_{ig}=2.69\%$ as presented in Figure 7 and 8.

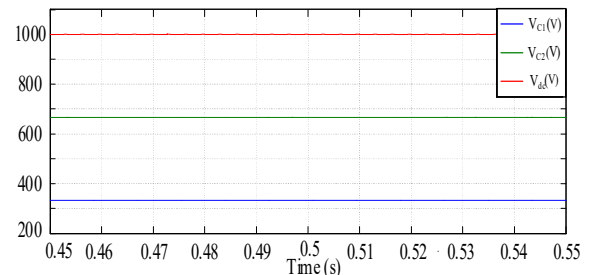


Fig. 4. Dc side and flying capacitors voltages in healthy mode

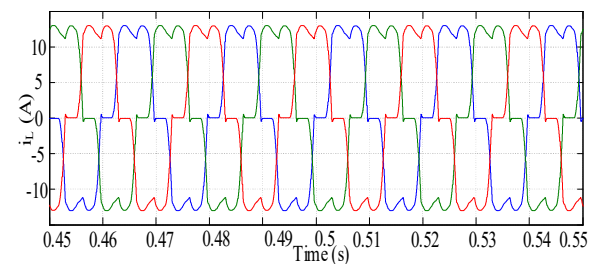


Fig. 5. Nonlinear load current in healthy mode

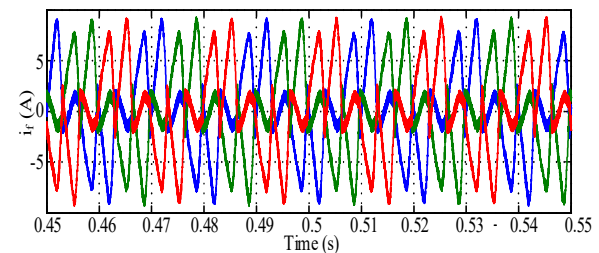


Fig. 6. Filter current in healthy mode

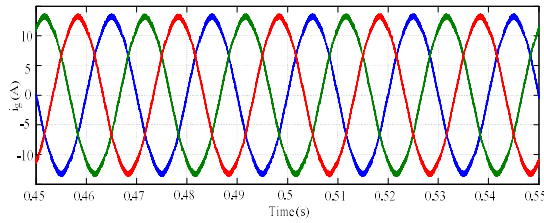


Fig. 7. Grid current in healthy mode

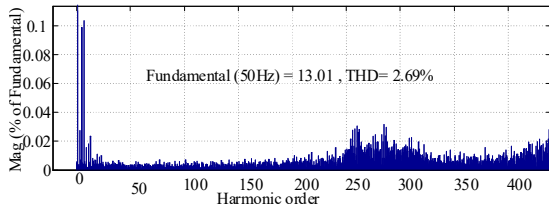


Fig. 8. Grid current in healthy mode

3.2. Failure of one flying capacitor

In this section, we consider the failure of C2 as shown in Figure 9.

The voltages V_{C1} and V_{C2} are not regulated to their desired values (Figure 10), also the multicellular converter injects faulty currents in the grid (Figure 11). Therefore, the grid current is not sinusoidal with $THD_{ig}=15.52\%$ (Figures 12 and 13) this THD value does not satisfies the IEEE limits.

The results confirm that the failure of one capacitor destabilize the active power filtering operation and make the multicellular converter affect the power quality instead of power quality improvement.

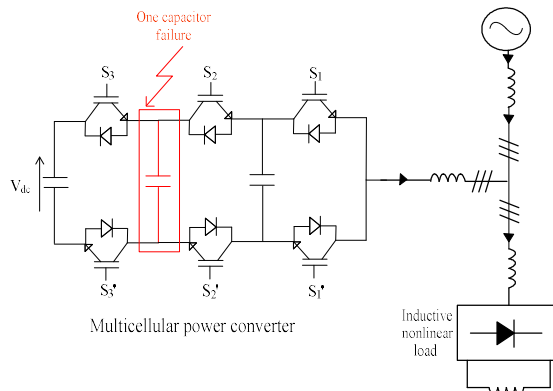


Fig. 9. One capacitor failure

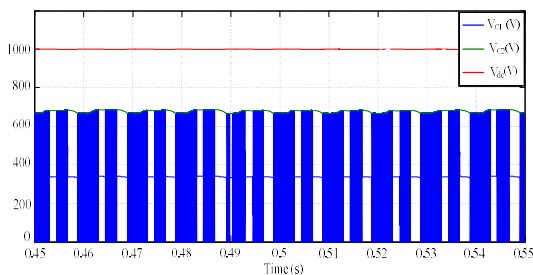


Fig. 10. DC side and flying capacitors voltages in one capacitor failure mode

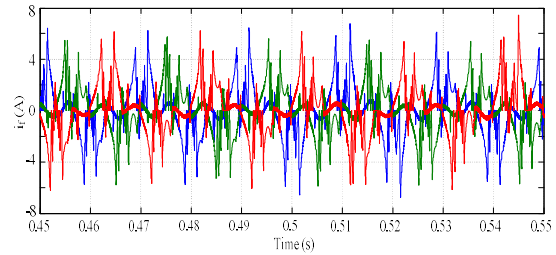


Fig. 11. Filter current under one flying capacitor failure

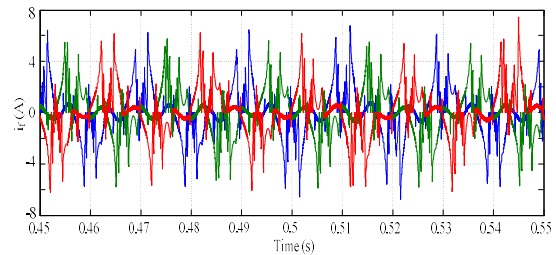


Fig. 12. Grid current in one capacitor failure mode

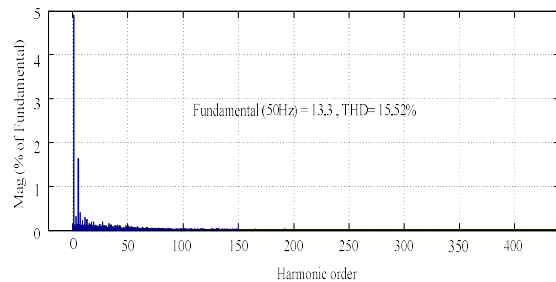


Fig. 13. THD of grid current under one flying capacitor failure

3.3. Two capacitor faults

In this section, the shunt active power filter based on multicellular converter has two failure capacitors as shown in figure 14.

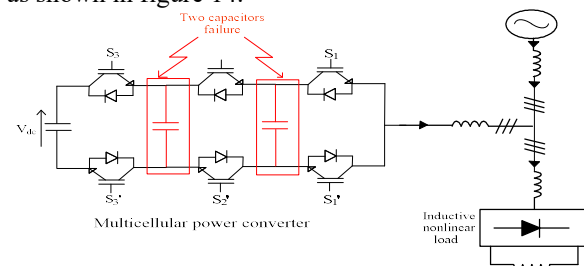


Fig. 14. Multicellular converter under two flying capacitors failure

Simulation results of shunt active power filter based on multicellular converter under two flying capacitors failure in (Figures 15-18) presents the divergence of V_{C1} and V_{C2} from their desired values and the multicellular converter injects the unwanted currents and affect the power quality of power grid with non-sinusoidal grid currents and high THD value ($THD_{ig}=15.70$), the spent coast in order to enhance the power quality with multicellular converter can affect the power quality and

destabilize the power grid in two flying capacitors failure mode.

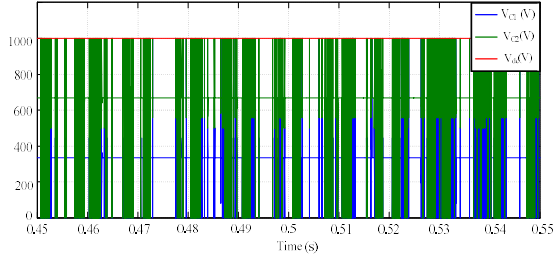


Fig. 15. Flying capacitors and dc side voltages in two capacitor failure mode

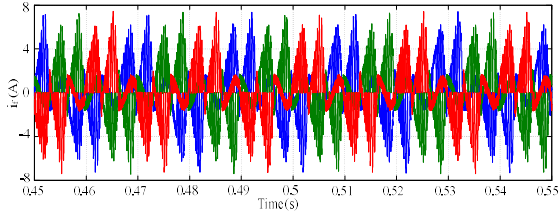


Fig. 16. Filter current in two capacitor failure mode

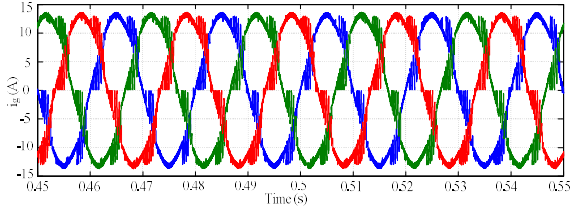


Fig. 17. Grid current in two capacitor failure mode

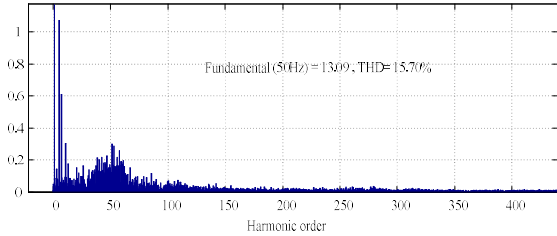


Fig. 18. THD of grid current under two flying capacitor failure

To enhance the power quality of power grid and optimize the cost of using shunt active power filter based on multicellular converter, a self-adaptive fault tolerant control is necessary without modify the topology of multicellular converter

3.4. Self-adaptive fault tolerant control

3.4.1. Failure of one flying capacitor

During the failure of C2, the elimination of second cell of multicellular converter by changing the control algorithm is necessary. Therefore, S_2 and S_3 have the same switching function. In this case, the equation 6 can be expressed by:

$$\begin{aligned} & \begin{bmatrix} \dot{V}_{C1} \\ \dot{i}_f \end{bmatrix} \\ &= \begin{bmatrix} 0 & 0 \\ 0 & -R_f \\ & L_f \end{bmatrix} \begin{bmatrix} V_{C1} \\ i_f \end{bmatrix} \\ &+ \begin{bmatrix} -(i_L - i_g) & (i_L - i_g) \\ \frac{C}{L_f} & \frac{C}{L_f} \end{bmatrix} \begin{bmatrix} S_1 \\ S_2 \end{bmatrix} \\ &+ \begin{bmatrix} 0 \\ -V_{dc} \\ \frac{V_g}{L_f} \end{bmatrix} \end{aligned} \quad (20)$$

$x = [V_{C1} \ i_f]^T$ is the state vector.

$x_{ref} = [\frac{V_{dc}}{2} \ i_{fref}]^T$ reference state vector.

$$f_{f1} = \begin{bmatrix} 0 & 0 \\ 0 & -R_f \\ & L_f \end{bmatrix}$$

$$g_f = \begin{bmatrix} -(i_L - i_g) & (i_L - i_g) \\ \frac{C}{L_f} & \frac{C}{L_f} \end{bmatrix}$$

$u = [s_1 \ s_2]^T$ input vector,

$$H = \begin{bmatrix} 0 \\ -V_{dc} \\ \frac{V_g}{L_f} \end{bmatrix} \text{ constant vector.}$$

where vector of error e is expressed by

$$e = x_{ref} - x = \begin{pmatrix} \frac{V_{dc}}{2} - V_{C1} \\ i_{fref} - i_f \end{pmatrix} \quad (21)$$

Equation 22-23 gives LYAPUNOV positive function and its derivative:

$$V = \frac{1}{2} e^T e \quad (22)$$

$$\dot{V} = e^T \dot{e} \quad (23)$$

$$\dot{V} = e^T (\dot{x} - \dot{x}_{ref})$$

Which can be expressed as:

$$\dot{V} = e^T (f(x) + g(x)u + H - \dot{x}_{ref}) \quad (24)$$

$$u = u_{eq} + u_n \quad (25)$$

$$u_{eq} = -(g(x))^{-1} (f(x) + H - \dot{x}_{ref}) \quad (26)$$

$$u = -(g(x))^{-1} (f(x) + H - \dot{x}_{ref}) + u_n \quad (27)$$

Substitution of equation 26 in equation 23

$$\dot{V} = e^T g(x) u_n \quad (28)$$

$$\dot{V} = e^T \left[\left(\frac{i_L - i_g}{C} + \frac{V_{C1}}{L_f} \right) S_1 + \left(\frac{i_L - i_g}{C} - \frac{(i_L - i_g)}{C} + \frac{V_{dc} - V_{C1}}{L_f} \right) S_2 \right] \quad (29)$$

In order to assure the stability of shunt active power filter the derivative of V must be negative.

$$S_1 = -\text{sign} \left[e^T \left(\frac{i_L - i_g}{C} + \frac{V_{C1}}{L_f} \right) \right] \quad (30)$$

$$S_2 = -\text{sign} \left[e^T \left(\frac{i_L - i_g}{C} - \frac{(i_L - i_g)}{C} + \frac{V_{dc} - V_{C1}}{L_f} \right) \right]$$

Figure 19 shows the sliding mode control of multicellular converter used in shunt active power filter during one capacitor failure mode.

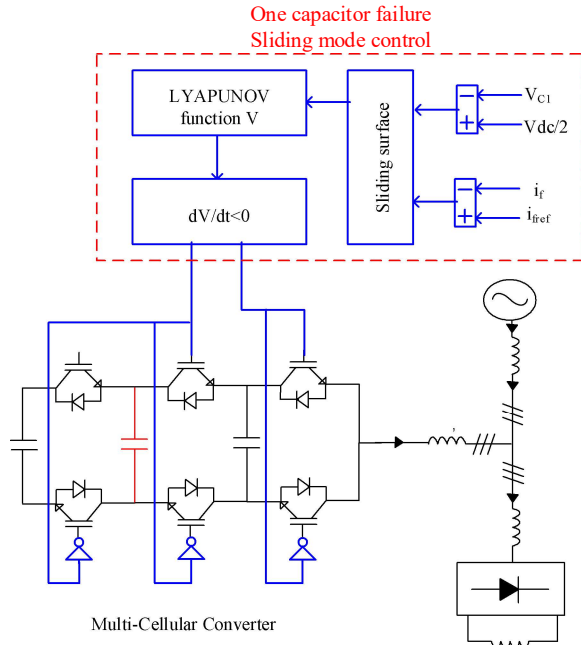


Fig. 19. Shunt active power filter with self-adaptive FTC and one capacitor failure mode

3.4.2. Simulation results during failure of one flying capacitor with FTC

In this section, the failure of C2 is considered, and the FTC is used. In simulation results, between 0.45s and 0.5s the shunt active power filter without FTC. After 0.5s, the self-adaptive FTC is applied by eliminating the cell with failure capacitor. with switching functions $S_2=S_3$.

During the application of self-adaptive FTC (instance 0.5s), V_{dc} regulates at its reference ($V_{dcref}=1000V$). V_{C1} regulates at its new reference ($V_{C1ref}=V_{dc}/2=500V$) as shown in Figure 20. Also, after 0.5s shunt active power filter generates the desired currents (Figure 21) and improve the form of grid current with $THD_{ig}=2.70\%$ (Figure 22 and figure 23).

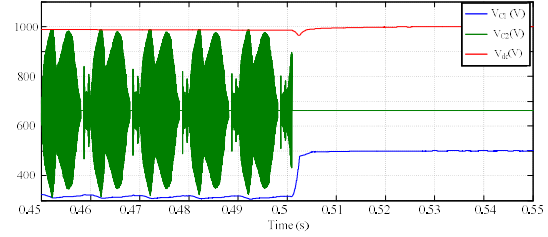


Fig. 20. DC side and flying capacitors voltages with self-adaptive FTC and one capacitor failure mode

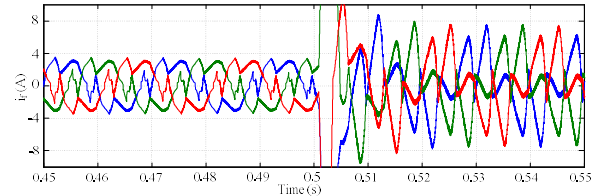


Fig. 21. Filter current with self-adaptive FTC and one capacitor failure mode

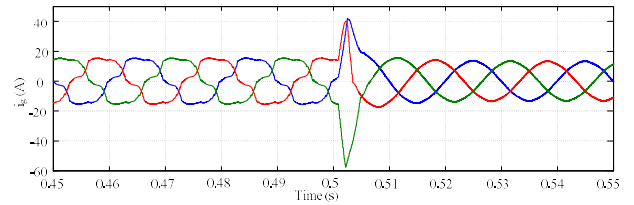


Fig. 22. Grid current with self-adaptive FTC and one capacitor failure mode

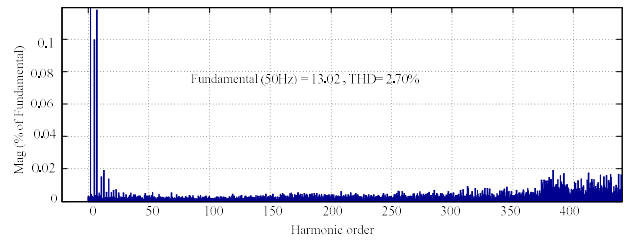


Fig. 23. THD of grid current with self-adaptive FTC and one capacitor failure mode

3.4.3. Failure of two capacitors

During the failure of two capacitors. Self-adaptive FTC based on hysteresis control is applied. In this case, $S_1=S_2=S_3$, therefore, the multicellular converter operates as two-level classical converter as presented in Figure 24.

3.4.4. Simulation results during failure of two capacitors failure with FTC

In this section, the failure of capacitors C1 and C2 is considered. Therefore, $S_1=S_2=S_3$ and multicellular converter operates as classical topology. at the instance 0.5s the self-adaptive FTC based on hysteresis control is applied. V_{dc} regulated at its desired value ($V_{dc}=V_{dcref}=1000V$) as shown in Figure 25, and the power quality is enhanced by injecting the desired current in the grid (Figure 26) and the grid current has a sinusoidal form (Figure 27) with acceptable THD (figure 29).

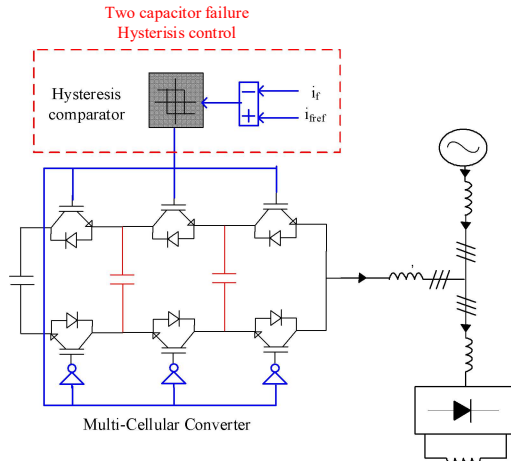


Fig. 24. Shunt active power filter with self-adaptive FTC and two capacitors failure mode

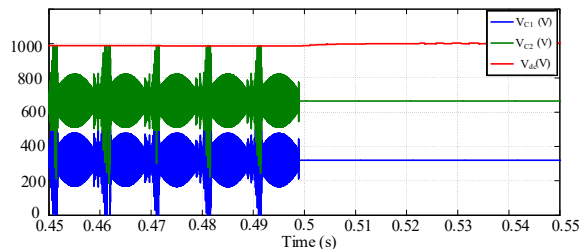


Fig. 25. DC side and flying capacitors voltages with self-adaptive FTC and two capacitors failure mode

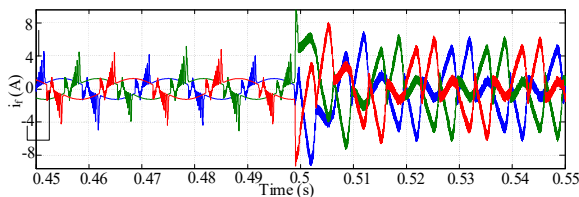


Fig.26. Filter current with self-adaptive FTC and two capacitors failure mode

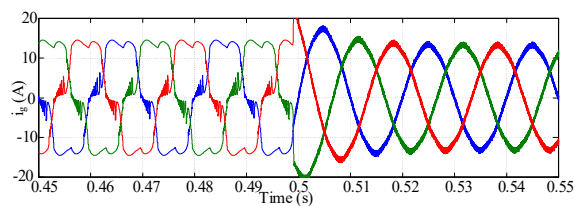


Fig. 27. Grid current with self-adaptive FTC and two capacitors failure mode

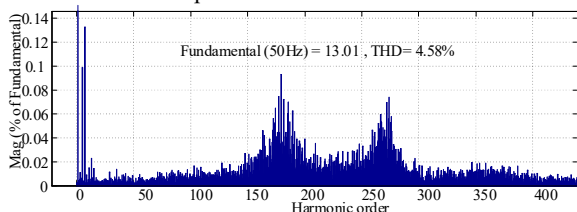


Fig. 29. THD of grid current with self-adaptive FTC and two capacitors failure mode

3.4.5. Comparison Between THD values for different state of multicellular converter

Table 2 gives the THD values of different state of multicellular converter compared to threshold of

IEEE-519, this table demonstrate the effectiveness of proposed self-adaptive FTC in power quality enhancement.

Table 2. THD values

Converter state	Threshold IEEE	Without FTC	With self-adaptive FTC
Healthy mode	5%	2.69%	2.69%
One capacitor failure	5%	15.52%	2.70%
Two capacitors failure	5%	15.70%	4.58%

3.5. Analysis of simulation results

In this paper, the proposed structure is shunt active power filter used to improve power quality of power grid. So, a sophisticated multicellular power converter and its control algorithm are used to have a sinusoidal grid current phase with grid voltage. However, according to the obtained results, during the failure of one or more flying capacitors, the THD of grid current exceeds the limits of the standards, and the multicellular converter becomes a source of instability instead of being a power enhancement tool. Therefore, the self-adaptive fault tolerant control (FTC) without changing the structure is applied. The obtained simulation results, proves that the FTC allows the multicellular converter with defected flying capacitor to enhance the power quality of power grid, this enhancement is justified by reducing the THD value of grid current under the threshold of standard as detailed in simulation results.

3.6. Benefits of society from this paper

The benefits of society from this paper are: Reduce the cost of failure in active power filter especially the proposed FTC does not require to changing the structure as well as optimize the energy consumption, extend the life time of electric machine in both domestic and industrial use.

4. CONCLUSION

This research paper represented a significant advancement in power quality enhancement and fault tolerant control in shunt active power filters. The proposed self-adaptive FTC was found to be highly robust and responsive to the dynamic conditions presented by the failure of flying capacitors, and preventing the injection of undesirable currents into the power grid.

The obtained simulation results provided solid evidence of the FTC's efficacy in enhancing power quality during fault scenarios. This research contributes to assure that power distribution systems adhere to the power quality standards and remain it reliable even in the face of component failures.

As further direction, we propose to deal with experimental validation of obtained results and apply this structure in smart grid system.

Source of funding: *No funding source.*

Author contributions: *research concept and design, A.B., B.R., M.R.K., L.L.; Collection and/or assembly of data, A.B., B.R., M.R.K., L.L.; Data analysis and interpretation, A.B., B.R., M.R.K., L.L.; Writing the article, ; Critical revision of the article, A.B., B.R., M.R.K., L.L.; Final approval of the article, A.B., B.R., M.R.K., L.L.*

Declaration of competing interest: *The authors declare that they have no known competing financial interests or personal relationships that could have appeared to influence the work reported in this paper.*

REFERENCES

- Mishra AK, Das SR, Ray PK, Mallick RK, Mohanty A, Mishra DK. PSO-GWO optimized fractional order pid based hybrid shunt active power filter for power quality improvements. *IEEE Access* 2020; 8: 74497–74512. <https://doi.org/10.1109/ACCESS.2020.2988611>.
- Song M, Fei W, Wang C, Liu X. design and study of a series active filter for the 10MW-level high power and high stability dc power supply. *IEEE Transactions on Applied Superconductivity* 2022; 32(6): 1–5. <https://doi.org/10.1109/TASC.2022.3172651>.
- Du X, Zhao C, Xu J. The Use of the hybrid active power filter in LCC-HVDC considering the delay-dependent stability. *IEEE Transactions on Power Delivery* 2022; 37(1): 664–673. <https://doi.org/10.1109/TPWRD.2021.3068411>.
- Fei J, Wang H. Experimental investigation of recurrent neural network fractional-order sliding mode control of active power filter. *IEEE Transactions on Circuits and Systems II: Express Briefs* 2020; 67(11): 2522–2526. <https://doi.org/10.1109/TCSII.2019.2953223>.
- Kale M, Özdemir E. Harmonic and reactive power compensation with shunt active power filter under non-ideal mains voltage. *Electric Power Systems Research* 2005; 74(3): 363–70. <https://doi.org/10.1016/j.epsr.2004.10.014>.
- Rouabah B, Toubakh H, Sayed-Mouchaweh M. Advanced fault-tolerant control strategy of wind turbine based on squirrel cage induction generator with rotor bar defects. *Annual Conference of the PHM Society* 2019; 11(1) <https://doi.org/10.36001/phmconf.2019.v11i1.841>.
- Mahboub MA, Rouabah B, Kafi MR, Toubakh H. Health management using fault detection and fault tolerant control of multicellular converter applied in more electric aircraft system. *Diagnostyka* 2022; 23(2): 1–7. <https://doi.org/10.29354/diag/151039>.
- Daramukkala P, Mohanty KB, Karthik M, Swain SD, Behera BP. Power quality enhancement using signed variable step size LMS adaptive filter-based shunt hybrid active power filter. *Sustainable Energy and Technological Advancements* 2023; 509–20. https://doi.org/10.1007/978-981-99-4175-9_41.
- Rouabah B, Toubakh H, Kafi MR, Sayed-Mouchaweh M. Adaptive data-driven fault-tolerant control strategy for optimal power extraction in presence of broken rotor bars in wind turbine. *ISA Transactions* 2022; 130: 92–103. <https://doi.org/10.1016/j.isatra.2022.04.008>.
- Chu Y, Luo X, Hou S, Fei J. Robust hybrid intelligent control using probabilistic feature for active power filter. *Control Engineering Practice* 2023; 141: 105712. <https://doi.org/10.1016/j.conengprac.2023.105712>.
- Akbari E, Zare Ghaleh Seyyedi A. Power quality enhancement of distribution grid using a photovoltaic based hybrid active power filter with three level converter. *Energy Reports* 2023; 9: 5432–48. <https://doi.org/10.1016/j.egyrs.2023.04.368>.
- Abou Houran M, Sabzevari K, Hassan A, Oubelaid A, Tostado-Véliz M, Khosravi N. Active power filter module function to improve power quality conditions using GWO and PSO techniques for solar photovoltaic arrays and battery energy storage systems. *Journal of Energy Storage* 2023; 72: 108552. <https://doi.org/10.1016/j.est.2023.108552>.
- Gautam S, Aeidapu M. sine cosine algorithm based shunt active power filter for harmonic compensation. 2019; 1051–1056. <https://doi.org/10.1109/ICECA.2019.8821800>.
- Rouabah B, Rahmani L, Mahboub MA, Toubakh H, Sayed-Mouchaweh M. More Efficient Wind Energy Conversion System Using Shunt Active Power Filter. *Electric Power Components and Systems* 2021; 49(4–5): 321–332. <https://doi.org/10.1080/15325008.2021.1970285>.
- Rachid D, Bassou A, Brahim F. The harmonics detection method based on neural network applied to harmonics compensation. *International Journal of Engineering, Science and Technology* 2010; <https://doi.org/10.4314/ijest.v2i5.60160>.
- Agrawal S, Kumar P, Palwalia DK. Artificial neural network based three phase shunt active power filter. 2016 *IEEE 7th Power India International Conference (PIICON)* 2016; 1–6. <https://doi.org/10.1109/POWERI.2016.8077153>.
- Mustapha S, Kamal D, Ghania B. Advanced control strategy based hybrid active power filter for power quality improvement. *ICENSOS* 2023; 1: 115–119.
- Koganti S, Koganti KJ, Salkuti SR. Design of multi-objective-based artificial intelligence controller for wind/battery-connected shunt active power filter. *Algorithms* 2022; 15(8): 256. <https://doi.org/10.3390/a15080256>.
- Baros J, Sotola V, Bilik P, Martinek R, Jaros R, Danys L. Review of fundamental active current extraction techniques for SAPF. *Sensors* 2022; 22(20): 7985. <https://doi.org/10.3390/s22207985>.
- Thirumoorthi P, Raheni TD. Artificial neural network controlled shunt active power filter for minimization of current harmonics in industrial drives. *International Journal of Innovative Technology and Exploring Engineering (IJITEE)* 2018; 8(2S): 150–155.
- Jain SK, Agarwal P. Design simulation and experimental investigations, on a shunt active power filter for harmonics, and reactive power compensation. *Electric Power Components and Systems* 2003; 31(7): 671–92. <https://doi.org/10.1080/15325000390203674>.
- Panda AK, Patnaik SS. Analysis of cascaded multilevel inverters for active harmonic filtering in distribution networks. *International Journal of Electrical Power & Energy Systems* 2015; 66: 216–26. <https://doi.org/10.1016/j.ijepes.2014.10.034>.

23. Barresi M, Ferri E, Piegari L. An MV-Connected Ultra-fast charging station based on MMC and dual active bridge with multiple dc buses. *Energies* 2023; 16(9): 3960. <https://doi.org/10.3390/en16093960>.
24. Noman AM, Alkuhayli A, Al-Shamma'a AA, Addoweesh KE. Hybrid MLI topology using open-end windings for active power filter applications. *Energies* 2022; 15(17): 6434. <https://doi.org/10.3390/en15176434>.
25. Jamil H, Qayyum F, Iqbal N, Kim DH. Enhanced harmonics reactive power control strategy based on multilevel inverter using ml-fnn for dynamic power load management in microgrid. *Sensors* 2022; 22(17): 6402. <https://doi.org/10.3390/s22176402>.
26. Figueroa F, Lizana Fuentes R, Goetz SM, Rivera S. Operation of a hybrid energy storage system based on a cascaded multi-output multilevel converter with a carrier-based modulation scheme. *Energies* 2023; 16(20): 7150. <https://doi.org/10.3390/en16207150>.
27. Wilkinson RH, Meynard TA, du Toit Mouton H. Natural balance of multicell converters: The two-cell case. *IEEE Transactions on Power Electronics* 2006; 21(6): 1649–57. <https://doi.org/10.1109/TPEL.2006.882958>.
28. Rouabah B, Rahmani L, Toubakh H, Duviella E. Adaptive and exact linearization control of multicellular power converter based on shunt active power filter. *Journal of Control, Automation and Electrical Systems* 2019;30. <https://doi.org/10.1007/s40313-019-00510-w>.
29. Rouabah B, Toubakh H, Djemai M, Ben-Brahim L, Kafi MR. New Active Fault tolerant control of multicellular converter. 2022 7th International Conference on Environment Friendly Energies and Applications (EFEA) 2022; 1–6. <https://doi.org/10.1109/EFEA56675.2022.10063825>.
30. Bouhafs A, Kafi MR, Louazene L, Rouabah B, Toubakh H. Fault-detection-based machine learning approach to multicellular converters used in photovoltaic systems. *Machines* 2022; 10(11): 992. <https://doi.org/10.3390/machines10110992>.
31. Rouabah B. Contribution à l'amélioration des performances d'un filtre actif parallèle de puissance par l'utilisation d'un convertisseur multicellulaire [Internet] [Thesis]. 2021.
32. Rouabah B, Toubakh H, Sayed-mouchaweh M. Fault tolerant control of multicellular converter used in shunt active power filter. *Electric Power Systems Research* 2020; 188: 106533. <https://doi.org/10.1016/j.epsr.2020.106533>.
33. Rouabah B, Toubakh H, Djemai M, Ben-Brahim L, Ghandour R. Fault diagnosis based machine learning and fault tolerant control of multicellular converter used in photovoltaic water pumping system. *IEEE Access* 2023; 11: 39013-39023. <https://doi.org/10.1109/ACCESS.2023.3266522>.



Ali BOUHAFS, Electrical: Engineering Laboratory (LAGE). Currently works at the Department of Electrical Engineering, Université Kasdi Merbah Ouargla. BOUHAFS does research in photovoltaic systems, photovoltaic solar pumping system, power converter Engineering, Control Systems Engineering and Electronic Engineering.

e-mail: bouhafs.ali@univ-ouargla.dz



Boubakeur ROUABAH, FNTIC Faculty, Kasdi Merbah University, currently works at the Department of Electronic and telecom. Boubakeur does research in power electronic converters, Control Systems and fault tolerant control.

e-mail: boubakeurrouabah@yahoo.fr



Mohamed Redouane KAFI, Electrical Engineering Laboratory (LAGE), currently works at the Electronic and telecom. Kafi does research in Aeronautical systems, Control of power systems and artificial intelligence.

e-mail: kafi.redouane@univ-ouargla.dz



Louazene LAKHDAR, Electrical Engineering Laboratory (LAGE) currently works as Head of Electrical Engineering Department, Université Kasdi Merbah Ouargla. Louazene Lakhddar does research in solar photovoltaic systems, photovoltaic solar pumping system, power converter Engineering, Control Systems Engineering and

Electronic Engineering.
e-mail: lakhdar.louazene@gmail.com